Water Air Soil Pollut (2020) 231: 190
https://doi.org/10.1007/s11270-020-04568-0

Permeability, Pore, and Structural Parameters of Undisturbed Silty Clay Presented in Landfill Leachate

Haijun Lu · Chaofeng Wang · Dinggang Li · Jixiang Li · Yong Wan

Received: 19 December 2019 / Accepted: 1 April 2020 / Published online: 18 April 2020

Abstract This study focused on the permeability and structural evolution of impeded soil layers in landfill. A series of laboratory tests including a permeability test, X-ray diffraction, nuclear magnetic resonance, scanning electron microscopy, and laser particle size tests were conducted to analyze the permeability and microstructure characteristics of undisturbed silty clay polluted by landfill leachate. The hydraulic conductivities increased with time in the first 108 h. After 108 h, the hydraulic conductivities of undisturbed silty clay polluted by landfill leachate decreased. After 205 h, the changes in the hydraulic conductivity stabilized, and the hydraulic conductivity decreased with the increase of the concentration of leachate. The volume fractions of inter-particle and intra-aggregate pores were much higher than those of other pores. The optimal radius decreased as the concentration of leachate increased. The blockage of the pore channel and weakened permeability was caused by solid matter interception by the porous medium. As the height of the specimen increased, the volume fraction of coarse grain changed rapidly and sharply, and the volume fraction of fine grain changed slowly. The average particle size increased with increased specimen height and decreased as the leachate concentration increased. A comprehensive structural parameter (ζ) of undisturbed silty clay polluted by landfill leachate was obtained based on the test results. The equation of comprehensive structural parameter ζ of undisturbed silty clay polluted by leachate was established. These results can provide fundamental data for evaluating the stability of the underlying stratum of landfill sites.

Keywords Undisturbed silty clay · Landfill leachate · Permeability · Pore · Particle size · Structural parameter

H. Lu (✉) · C. Wang · D. Li · J. Li
School of Civil Engineering and Architecture, Wuhan Polytechnic University, Wuhan 430023, China
e-mail: lhj_whpu@163.com

C. Wang
e-mail: wangchaofeng1010@126.com

D. Li
e-mail: Lidinggang1992@163.com

J. Li
e-mail: jixiangli@whpu.edu.cn

Y. Wan (✉)
State Key Laboratory of Geomechanics and Geotechnical Engineering, Institute of Rock and Soil Mechanics, Chinese Academy of Sciences, Wuhan 430071, China
e-mail: wy_cersm@163.com

1 Introduction

Xue et al. (2013) and Li et al. (2016) have shown that completely impermeable landfill liner systems are rare in China, and thus garbage in landfill is always directly positioned onto the underlying stratum. Landfill leachate contains considerable levels of heavy metal ions and organic pollutants, and the occurrence of leakage causes many engineering problems, such as uneven settlement and instability in landfill. Additionally, contaminant

migration to landfill leachate is a complex process. Thus, determination of the permeability laws of the underlying stratum and the corresponding microstructure behaviors under the landfill leachate is a key to predicting destruction of the landfill foundation.

A series of studies focused on the permeability and microstructure characteristics of contaminated soil have been carried out. Francisca and Glatstein (2010) and Li et al. (2013a) found that pore clogging decreased both effective porosity and hydraulic conductivity. Li et al. (2013b) discovered that the changes of particle fabrics affect the hydraulic conductivity of kaolin by clogging the pore spaces with bio-slurry. Nayak et al. (2007) found that the clay contaminated by landfill leachate positively affected the porosity and the hydraulic conductivity of clay, and the maximum dry density of clay decreased. VanGulck and Rowe (2004) found that the drainage porosity began to decrease from 0.38 to 0.1 after the removal of steady chemical oxygen demand, causing a decrease of the hydraulic conductivity by five orders of magnitude. Guyonnet et al. (2005) indicated that there were connections among the hydraulic conductivity, the proportions of gel phase, and clay inter-layer occupation of sodium. Hou et al. (2017) found that the corrosion behavior of landfill leachate upgraded the gel structure of stabilized clay, with the small pores becoming larger, and the original "face–face" connection was converted into "face–edge" or "edge–edge" connection. Previous studies on contaminated soil have mainly focused on the remolded soil. Some other scholars (Chen et al. 2011; Xie et al. 2009a, b, 2015, 2018; Zhan et al. 2014) measured and calculated the contents of organic pollutants, chlorides, Na, COD, and heavy metals at the bottom of the geosynthetic clay liner for different regions, and based on the hydraulic model, considered the effects of water content and migration of organic pollutants on landfill sites. However, to our knowledge, there are a few studies on comprehensive structural parameters for hydraulic conductivity and pore change test results of undisturbed silty clay polluted by landfill leachate. Furthermore, it is difficult to obtain detailed information about soil microstructure parameters; therefore, it is necessary to find a comprehensive structural parameter that can reflect the evolution of structural characteristics in soil polluted by leachate.

In this study, the evolution laws of the permeability, pore, size distribution, and microstructure characteristics of undisturbed silty clay polluted by landfill leachate were systematically examined using methods such as permeability, nuclear magnetic resonance (NMR), X-ray diffraction (XRD), scanning electron microscopy (SEM), and laser particle size (LPS) tests. This study aimed to reveal the laws of permeation characteristics and the structural evolution for undisturbed silty clay and comprehensive structural parameters, providing fundamental data for assessing the underlying stratum of landfill.

2 Materials and Methods

2.1 Materials

Undisturbed silty clay was taken from a simple landfill site in Huangpi District, Wuhan, China based on the "Technical standard for sampling of undisturbed soils" (JGJ 89-1992, 1993) and "Specification of soil test" (SL 237-1999, 1999) methods. The soil sampling instrument is SD soil sampling drill (Beijing Tethys Technology Co., Ltd., China), and soil sample is sealed and transported to the laboratory. The natural density, moisture content, specific gravity, plastic limit, and liquid limit are 2.10 g/cm^3, 15.6%, 2.68, 18.8%, and 34.4%. The mineral composition of undisturbed silty clay is shown in Fig. 1, mainly including illite, albite, montmorillonite, muscovite, kaolinite, and quartz. The landfill leachate, aged 3 years, was collected from Chenjiachong landfills, Wuhan, China. Table 1 shows chemical parameters of landfill leachate used as permeating liquid. Three solutions with different concentrations were used in the test by dilution with distilled water: 16.7% (volume ratio of distilled water and leachate of 5:1), 50% (volume ratio of distilled water and leachate of 1:1), and 100% (leachate only).

2.2 Methods

The undisturbed silty clay specimens (diameter = 50 mm and height = 100 mm) were pre-saturated in a vacuum saturating cylinder. According to the US test standard ASTM D5084-03, hydraulic conductivity was measured by an environmental geotechnical flexible wall permeameter PN3230M (GEOEQUIP, America). The penetrant liquids were leachate with concentrations of 16.7%, 50%, and 100%. The confining pressure and back pressure were 350 and 100 kPa. The hydraulic conductivity was calculated by the following equation:

$$K = \frac{Q \cdot H \cdot \rho \cdot g}{10^5 \cdot A \cdot t \cdot P} \quad (1)$$

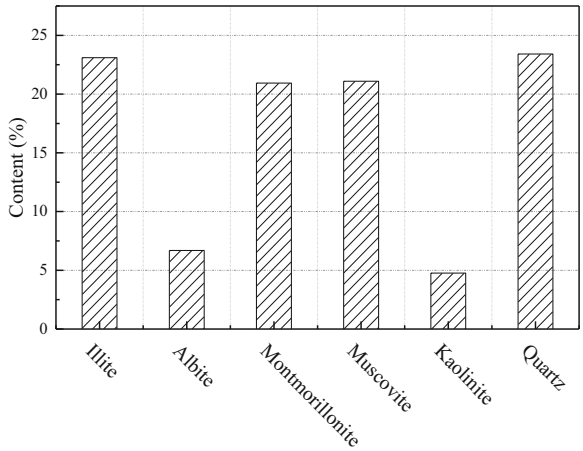

Fig. 1 Mineral composition of undisturbed silty clay

where K is the hydraulic conductivity (cm/s), Q is the collected leachate at time t (m^3), H is the height of the specimen (mm), ρ is the leachate density (kg/m^3), g is the ratio of gravity and quality (m/s^2), A is the cross-sectional area of the specimen (cm^2), t is the permeation time (s), and P is the applied water head (kPa).

2.2.1 XRD Tests

After the permeability tests, each specimen was divided into five layers on average from bottom to top, each layer being about 2 cm. The specimens (about approximately 200 g) used in the XRD tests were taken from the bottommost 0–2 cm of specimens after the permeability test was finished. The specimens were air dried, crushed, and passed through a 0.075 mm sieve. The mineral compositions of specimens were obtained with an EMPYREAN diffractometer (PANalytical B.V., the Netherlands).

2.2.2 NMR Tests

The pore radius was measured based on the soil–water characteristic curve in the NMR test (Tian et al. 2013). The specimens (2 mm × 2 mm × 2 mm) used in NMR tests were taken from the 0–2, 4–6, and 8–10 cm layers of the specimens after permeability test was finished.

2.2.3 SEM Tests

The specimens (1 mm × 1 mm × 1 mm) used in the SEM tests were taken from the bottommost 0–2 cm of specimens and immediately air dried after the permeability test was finished. The magnification of the SEM images was 2000 times. The tests were repeated at least three times to produce representative data.

2.2.4 LPS Tests

The specimens used in the LPS tests were taken from the 0–2, 4–6, and 8–10 cm layers of specimens after the permeability test was finished. The soil specimens (300 g) were air dried, crushed, and passed through a 0.075 mm sieve. Particle size characteristics were tested with a Malvern Mastersizer 3000 laser particle size analyzer, and the LPS test was conducted for three groups of parallel tests at the same concentration.

3 Results and Discussion

3.1 Penetration Properties and Mineral Composition

Figure 2 shows the changes in the hydraulic conductivity of the undisturbed silty clay over time. The hydraulic

Table 1 Chemical parameters of landfill leachate used as permeating liquid

Parameters	Range	Determination method	Parameters	Range	Determination method
pH	6.0–6.3	GB/T 6920-86	COD	642–4317	HJ/T 399-2007
DO	13–71	GB/T 7489-87	TOC	108–795	HJ 501-2009
$N\text{-}NO_3$	15–52	HJ/T 346-2007	SO_4^{2-}	17–64	GB/T 13196-91
$N\text{-}NO_2$	6–43	HJ/T 197-2005	Cl^-	544–2360	GB/T 11896-89
$N\text{-}NH^{4+}$	802–4163	HJ 666-2013	Na^+	595–2172	GB/T 11903-89
$P\text{-}PO_4$	26–91	HJ 669-2013	Zn	73–348	GB 7472-1987
TP	12–27	HJ 671-2013	Cu	209–926	HJ 485-2009
BOD_5	403–1744	HJ 505-2009	Ni	104–473	GB 11912-1989

All parameters are expressed in mg L^{-1}, except pH

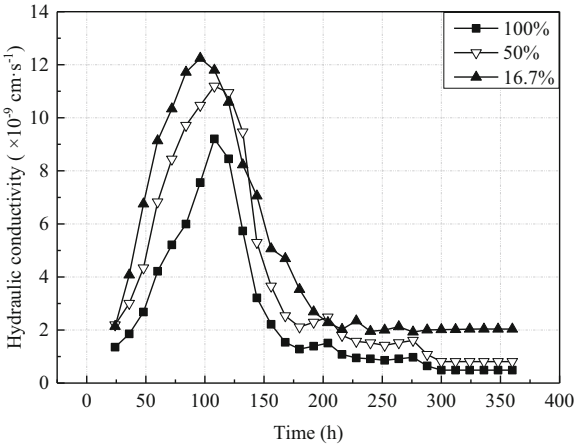

Fig. 2 Change in hydraulic conductivity of undisturbed silty clay with time

conductivities increased in the first 108 h. After 108 h, the hydraulic conductivity decreased until it eventually stabilized at 205 h (Fig. 2). Moreover, when the penetrant liquids were leachate with concentrations of 16.7%, 50%, and 100%, the hydraulic conductivities were 2.034×10^{-9}, 8.088×10^{-10}, and 4.872×10^{-10} cm/s, respectively.

The above phenomena may have occurred because the leachate damaged the structure of the soil and simultaneously reorganized the soil particles, some of which became suspended. In addition, landfill leachate had a negative influence on the thickness of the adsorbed layer (Amadi and Eberemu 2011), and the porosity of undisturbed silty clay increased. In the initial stages of the permeability test, the total porosity in the undisturbed silty clay and the hydraulic conductivity increased over time. In the final stage, negatively charged soil particles became bigger because leachate contains a large amount of heavy metal ions. A large number of insoluble solid particles and organic substances in leachate adhere to the surface, blocking the connected pores, resulting in a decrease in porosity (Ozcoban et al. 2013). Organic pollutants in leachate are degraded by microorganisms, and insoluble sediments start to block pores, resulting in the decrease of the hydraulic conductivity over time. However, although the specimen prepared at high concentration leachate had higher porosity than the specimen at low concentration, the permeability value was lower (Oztoprak and Pisirici 2011). Therefore, the hydraulic conductivity decreased when the concentration of landfill leachate increased.

Figure 3 presents the mineral contents of undisturbed silty clay polluted by leachate at different concentrations. The contents of quartz and muscovite changed only minimally, whereas the contents of illite and montmorillonite decreased by 23.34% and 23.14%, respectively. This indicates that some of the clay minerals in soil granules were dissolved during leachate infiltration and the arrangement and size of soil particles had changed. Therefore, the hydraulic conductivity also decreased with the increase of the leachate concentration.

3.2 Pore Characteristics

The transverse relaxation time (T_2) provided by the Carr–Purcell–Meiboom–Gill sequence was obtained from the NMR tests. The T_2 distribution curves for undisturbed silty clay in contact with leachate with concentrations of 16.7%, 50%, and 100% are shown in Figs. 4, 5, 6, respectively. The first area between the T_2 distribution curve and lateral axis was defined as the first peak area and represented the water content from leachate. The second peak area represented organic matter content from landfill leachate (Gao et al. 2009). According to Figs. 4, 5, 6, the first peak area increased with the increase of the concentration of landfill leachate and specimen height. The leachate introduced various heavy metal ions and organic pollutants into the undisturbed silty clay, which affected the cementation and flocculation structure of the undisturbed silty clay surface between the soil particles or between the layers of clay minerals, causing this substantial change in soil structure.

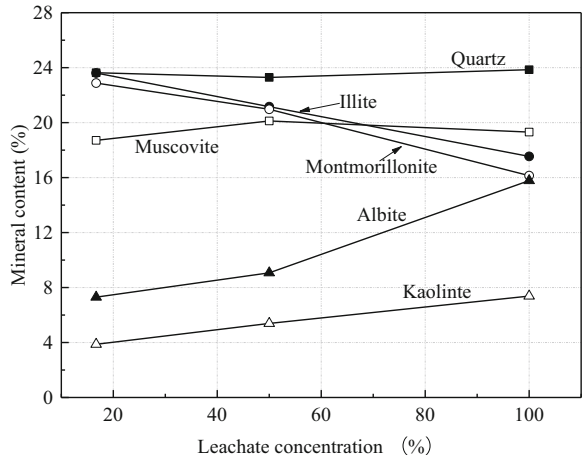

Fig. 3 The mineral content for undisturbed silty clay polluted by landfill leachate

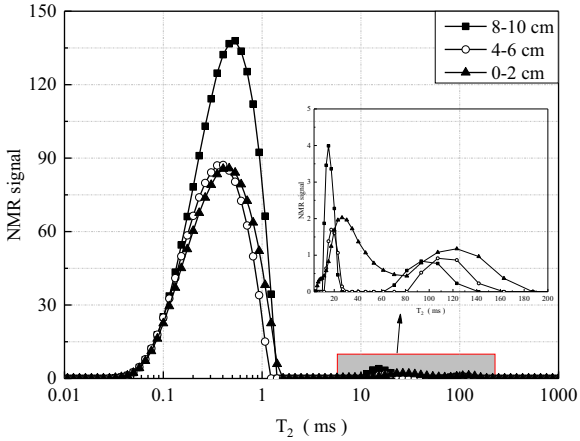

Fig. 4 T_2 distribution curves for undisturbed silty clay polluted by landfill leachate (16.7%)

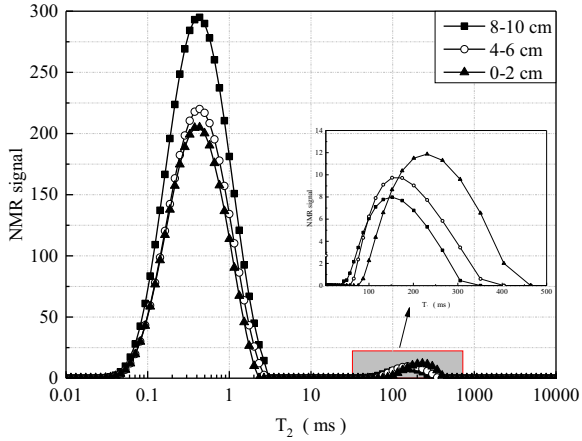

Fig. 6 T_2 distribution curves for undisturbed silty clay polluted by landfill leachate (100%)

The pore size distribution curves for undisturbed silty clay in contact with different concentrations of landfill leachate are shown in Figs. 7, 8, 9. The optimal radius was the value of the radius at the maximum NMR signal. The volume fraction of inter-particle and intra-aggregate pores was much higher than that of other pores. The optimal radius decreased with the increase of the concentration of landfill leachate. When the leachate concentration was 100%, the optimal radius of the pores was 0.19 μm. At the same concentration, the optimal radius of different heights was roughly the same. In general, the volume fraction of pores increased with the increase of leachate concentration.

The above results suggest that landfill leachate contained many organic pollutants and heavy metal ions, which can corrode undisturbed silty clay by various biological, physical, and chemical means, resulting in an increase in hydraulic conductivity (De Soto et al. 2018; Liu and Hu 2014). These large particles were reduced in size by corrosion, resulting in a larger specific surface area and an increased adsorption capacity. The blockages in the pore channels and the weakened permeability occurred because the generated tiny solid matter was intercepted by the porous medium. The organic contaminants were effectively retarded in the soil layer that first made contact with the leachate; thus, the content of organic contaminants in the next soil layer decreased substantially (Lu et al. 2015).

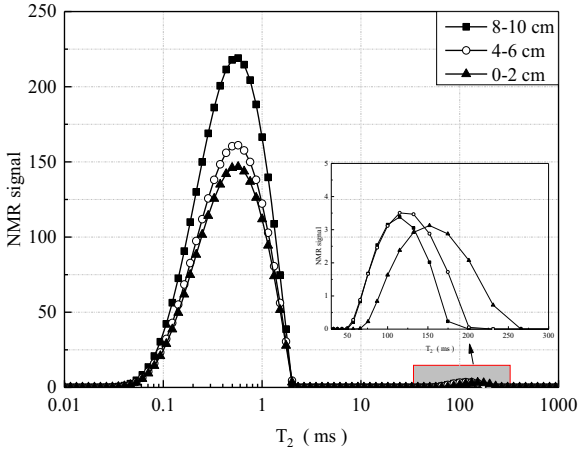

Fig. 5 T_2 distribution curves for undisturbed silty clay polluted by landfill leachate (50%)

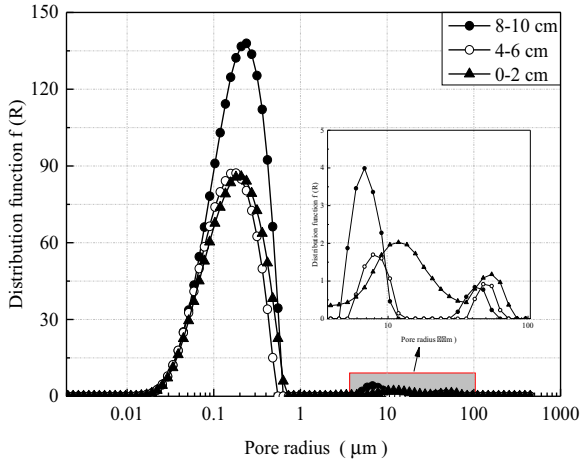

Fig. 7 Pore size distribution curves of undisturbed silty clay polluted by landfill leachate (16.7%)

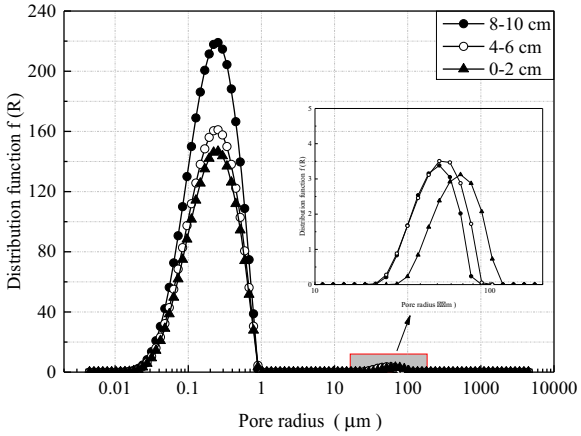

Fig. 8 Pore size distribution curves of undisturbed silty clay polluted by landfill leachate (50%)

3.3 Qualitative and Quantitative Analysis of Microstructures

The SEM images of soil specimens are shown in Fig. 10. Figure 10A reveals that there are many small pores in the specimen and the surface of soil specimen was rough and had a large amount of flaky substances attached to it. In Fig. 10B, the soil structure appeared to be mostly unstable honeycomb, and a large number of micro-pores were apparent from the surface. In Fig. 10C, there are few pores on surface of the sample, and the soil structure is granular and flaky, which indicates that high leachate concentration easily caused pore blockage; at the same time, the number of micro-pores reduced substantially according to the penetration test. Therefore, the hydraulic conductivity decreased at a

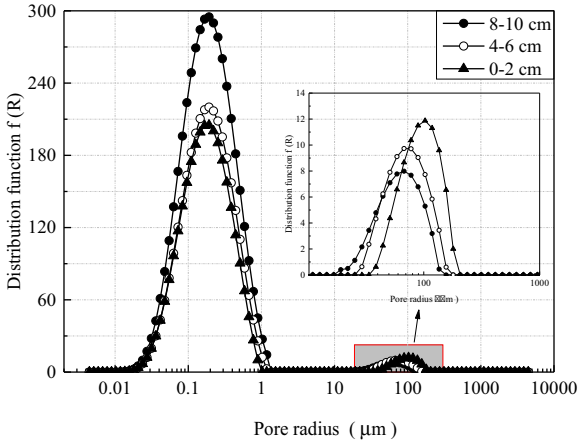

Fig. 9 Pore size distribution curves of undisturbed silty clay polluted by landfill leachate (100%). **A** 16.7%. **B** 50%. **C** 100%

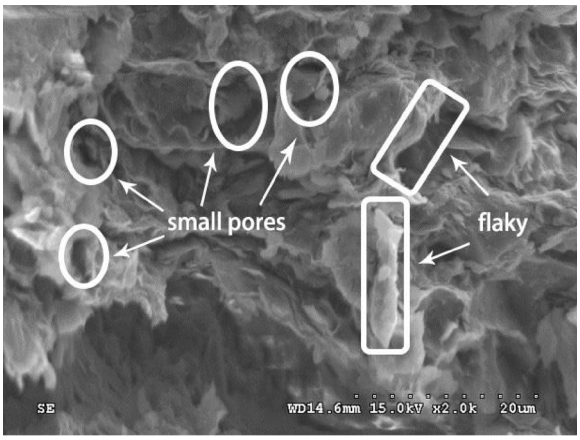

(a) 16.7%

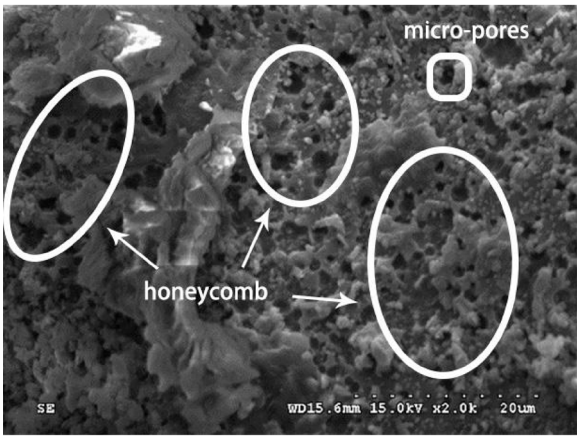

(b) 50%

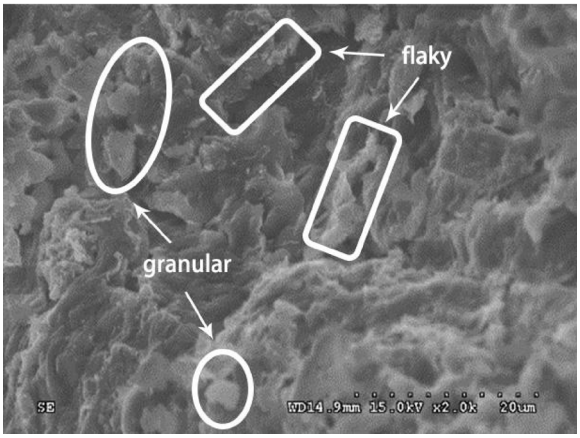

(c) 100%

Fig. 10 SEM images of undisturbed silty clay polluted by 100% landfill leachate after permeability test. **A** 16.7%. **B** 50%. **C** 100%

macroscopic level as the leachate concentrations increased. The SEM images of soil sample conform to

the variation rule of hydraulic conductivity obtained from permeability test.

Figure 11 shows the particle size curves of soil specimens. When the height of the specimen increased, the particle size distribution curve of undisturbed silty clay showed "thin and high" style. The volume fraction of coarse grain changed rapidly and quickly. Moreover, the volume fraction of fine grain changed slowly. This could be because the structural links of soil particles polluted by landfill leachate became weakened, resulting in the destruction of the aggregate structure in the soil (Qiang et al. 2014). The soil aggregates were dispersed into small soil particles, which were easily taken away by leachate (De Soto et al. 2012). The effect of this phenomenon on coarse particles was more apparent. Therefore, the coarse particles reduced rapidly, resulting in an increase of fine particles at different scales.

Figure 12 reveals the average particle size and specific surface area of the soil specimens. The average particle size increased when the height of the specimen increased and decreased when the leachate concentrations increased. In the 8–10 cm layer of the specimen, the average particle size of the specimen polluted by 16.7% and 50% landfill leachate decreased by 43.71% and 45.99%, respectively. However, the average particle size of specimen polluted by 100% landfill leachate decreased by only 22.91%, indicating that high leachate concentrations had less influence on the soil particle decomposition than low concentrations. In the 8–10 cm layer of the specimen, different concentrations of landfill leachate had less influence on the damage degree of soil particle size. Additionally, the specific surface area decreased and increased when the height of the specimen and leachate concentrations increased, respectively. The changes in the macroscopic mechanical behavior of undisturbed silty clay in landfill leachate were related to the reduction of porosity and interparticle volume (Qiang et al. 2014).

According to the LPS test results, the particle size and $D_v(50)$ of undisturbed silty clay with a volume distribution of 50% are known. Figure 13 shows the $D_v(50)$ and span of the soil specimens. The change of $D_v(50)$ was the same as the change in the average particle size. However, the span decreased when the height of the specimen, and the leachate concentrations increased. The change of span in the 0–6 cm layer of the specimen was greater than that in the 6–

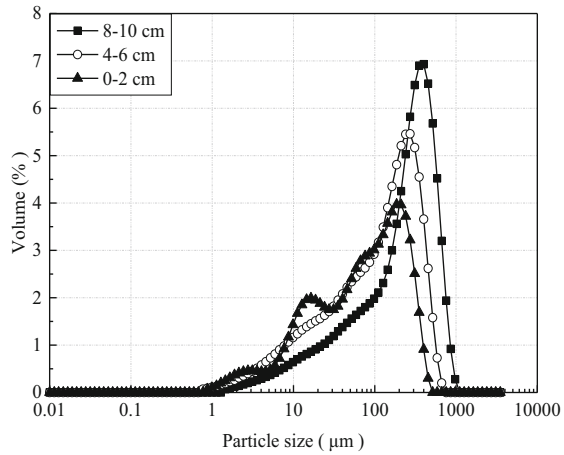

(a) 16.7%

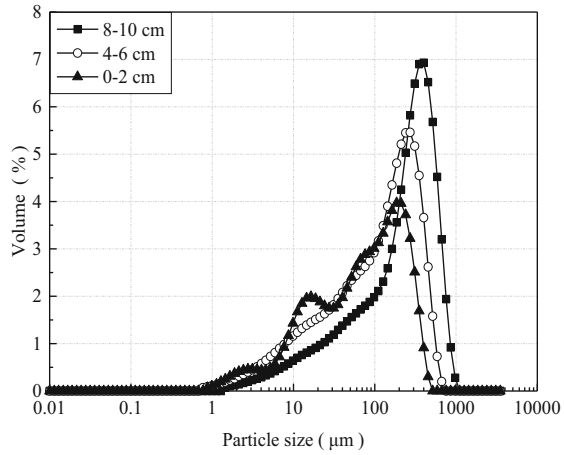

(b) 50%

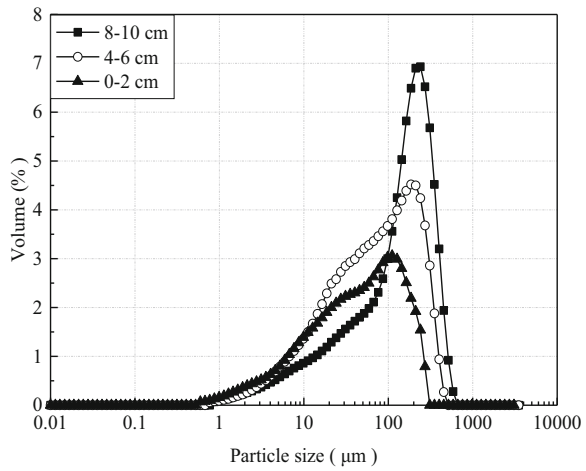

(c) 100%

Fig. 11 Particle size curve of undisturbed silty clay polluted by landfill leachate

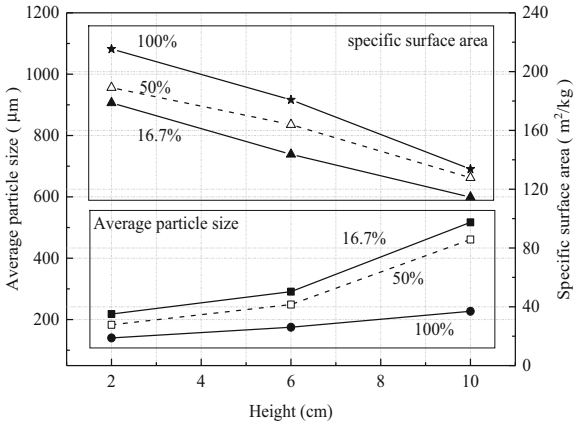

Fig. 12 Average particle size and specific surface area of undisturbed silty clay polluted by landfill leachate

10 cm layer of the specimen. This was because the organic pollutants in leachate reacted with minerals in the soil, decreasing the soil particle size, and thus, the particle distribution width in undisturbed silty clay decreased because of the uniformity in particle. As the leachate concentration increased, the specific surface area of the undisturbed silty clay increased, and thus, the adsorption also increased, leading to an increase in organic matter of soil with an increase in leachate concentrations. The organic pollutants at high concentrations of leachate had a strong inhibition effect on the microstructure.

3.4 Comprehensive Structural Parameters

The previous analysis revealed that the leachate pollution resulted in many changes including the size, shape, and arrangement of soil particles, the pore size, and the hydraulic conductivity. Therefore, the average particle size, maximum pore size, $D_v(50)$, and span were selected for comprehensive quantitative evaluation.

In this paper, the microstructure parameters of undisturbed silty clay contaminated by leachate were evaluated based on principal component analysis (PCA). The microscopic parameters obtained from the above experiments are shown in Table 2. The data in Table 2 were used to generate the Z-score with the following equation:

$$x_{i'} = \frac{x_i - \overline{x}}{\sigma} \tag{2}$$

where $x_{i'}$ is the new standardized data, x_i is the raw data, $\overline{x}$ is the average value of specimen data, and σ is standard deviation of specimen data. The generated Z-scores are shown in Table 3.

The specimen correlation matrix R was obtained as follows:

$$R = \begin{pmatrix} 1 & -0.701 & 0.907 & -0.481 \\ -0.701 & 1 & -0.700 & 0.027 \\ 0.907 & -0.700 & 1 & -0.566 \\ -0.481 & 0.027 & -0.566 & 1 \end{pmatrix} \tag{3}$$

$$|R - \lambda I_4| = 0 \tag{4}$$

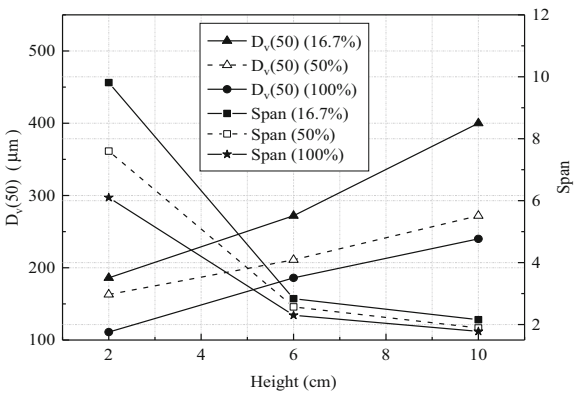

Fig. 13 $D_v(50)$ and span of undisturbed silty clay polluted by landfill leachate

Table 2 The microscopic parameters of undisturbed silty clay polluted by leachate

Specimens	Average particle size/μm x_1	Maximum pore/μm x_2	$D_v(50)$ /μm x_3	Span x_4
1	218	72.76	186	9.813
2	291	63.28	272	2.835
3	517	55.04	400	2.157
4	183	103.14	163	7.6
5	249	89.70	211	2.57
6	461	78.01	272	1.89
7	140.1	179.42	111	6.1
8	175	156.05	186	2.3
9	227	135.73	240	1.78

Table 3 The Z-score micro-parameters

Component Serial number	x_1	x_2	x_3	x_4
1	− 0.42488	− 0.70674	− 0.49038	1.92440
2	0.13442	− 0.92333	0.54383	− 0.43276
3	1.86594	− 1.11170	2.08313	− 0.66179
4	− 0.69304	− 0.01255	− 0.76698	1.17685
5	− 0.18737	− 0.31956	− 0.18974	− 0.52227
6	1.43689	− 0.58657	0.54383	− 0.75198
7	− 1.02172	1.73107	− 1.39232	0.67016
8	− 0.75433	1.19696	− 0.49038	− 0.61348
9	− 0.35592	0.73242	0.15901	− 0.78914

Four nonnegative eigenvalues could be obtained from the eigenvalue Eq. (4) of matrix R: $\lambda_1 = 2.779$, $\lambda_2 = 0.977$, $\lambda_3 = 0.165$, and $\lambda_4 = 0.079$. The total variance explained of matrix R is shown in Table 4. The variance contribution rate of α_1 was 69.479%, which was much larger than the variance contribution rate of α_2, α_3, and α_4. Therefore, more comprehensive micro-information was calculated by selecting the comprehensive structural parameters that reflect the eigenvalues and eigenvectors of α_1.

The structural parameter (ζ) of undisturbed silty clay under leachate infiltration was obtained by principal component analysis (PCA) in Statistic Package for Social Science (SPSS) multivariate statistics. The loadings of the variables for each component in the calculation process are shown in Table 5, and the equation is as follows:

$$\zeta = 0.572x_1 - 0.460x_2 + 0.583x_3 - 0.347x_4 \quad (5)$$

where ζ is the structural parameter, x_1 is the average particle size, x_2 is the maximum pore size, x_3 is $D_v(50)$, and x_4 is the span.

Table 5 Loadings of the variables for each component

Loadings	Comp 1	Comp 2	Comp 3	Comp 4
x_1	0.572	0	0.637	0.515
x_2	− 0.460	− 0.593	0.626	− 0.211
x_3	0.583	0	0.127	− 0.802
x_4	− 0.347	0.803	0.432	− 0.217

The ζ of undisturbed silty clay was positively correlated with $D_v(50)$ and the average particle size; however, it also had a negative correlation with the maximum pore and span. The absolute coefficients of the average particle size and $D_v(50)$ were larger than those of the maximum pore and span.

According to hydraulic conductivities obtained through experiments and the calculated results of structural parameters, when the penetrant liquids are leachate with concentrations of 16.7%, 50%, and 100%, the hydraulic conductivities (K) are 2.034×10^{-9}, 8.088×10^{-10}, and 4.872×10^{-10} cm/s, and the calculated results of structural parameters ζ are 198.801, 151.713, and 80.574, respectively. When the hydraulic conductivity decreases, the value of the comprehensive structural parameter ζ also decreases, which indicates that there is a strong correlation between microstructure parameters and hydraulic conductivities. The comprehensive structural parameters obtained through average particle size, maximum pore size, $D_v(50)$, and span can be used as a reference for evaluating the permeability characteristics of undisturbed silty clay corroded by landfill leachate.

4 Conclusions

A series of microstructure laboratory tests (XRD, NMR, SEM, and LPS tests) and permeability tests were performed

Table 4 Total variance explained of matrix R

Component	Initial eigenvalue			Extraction sums of squared loadings		
	Total	% of Variance	Cumulative %	Total	% of Variance	Cumulative %
x_1	2.779	69.479	69.479	2.779	69.479	69.479
x_2	0.977	24.419	93.898			
x_3	0.165	4.115	98.013			
x_4	0.079	1.987	100.000			

to evaluate the mineral composition, pore characteristics, surface morphology, particle size distribution, and the permeability of undisturbed silty clay polluted by different concentrations of landfill leachate. Based upon the test results and analyses, the following conclusions were drawn:

1. The hydraulic conductivities (K) of undisturbed silty clay increased with time in the first 108 h, and then the hydraulic conductivity decreased and tended to stabilize at 2.034×10^{-9}, 8.088×10^{-10}, and 4.872×10^{-10} cm/s at 16.7%, 50%, and 100% of the leachate concentration, respectively. The hydraulic conductivity can meet the engineering requirements of 1×10^{-7} cm/s for the landfill impervious layer.
2. When the leachate concentration increased from 16.7 to 100%, the contents of quartz and muscovite showed little change, whereas the content of illite and montmorillonite decreased by 23.34% and 23.14%, respectively. The optimal pore radius of undisturbed silty clay decreased as the landfill leachate concentration increased, and the volume fraction of pores showed a trend opposite to that of the optimal pore radius.
3. The volume fraction of coarse grain increased sharply, whereas the volume fraction of fine grain decreased with an increase of the height of the soil specimen. The average particle size increased when the height of the specimen increased and decreased when the leachate concentrations increased. However, the span decreased when the height of the specimen and the leachate concentrations increased.
4. The comprehensive structural parameters (ζ) of undisturbed silty clay were obtained by PCA on the basis of the value of the average particle size, maximum pore size, *Dv(50)*, and span. The equation of comprehensive structural parameter ζ of undisturbed silty clay polluted by leachate was established.

References

Amadi, A. A., & Eberemu, A. O. (2011). Performance of cement kiln dust in stabilizing lateritic soil contaminated with organic chemicals. *Advanced Materials Research, 367*, 41–47. https://doi.org/10.4028/www.scientific.net/AMR.367.41.

Chen, Y., Xu, X., & Zhan, L. (2011). Analysis of solid-liquid-gas interactions in landfilled municipal solid waste by a bio-hydro-mechanical coupled model. *Science China Technological Sciences, 55*(1), 81–89. https://doi.org/10.1007/s11431-011-4667-7.

De Soto, I. S., Ruiz, A. I., Ayora, C., García, R., Regadio, M., & Cuevas, J. (2012). Diffusion of landfill leachate through compacted natural clays containing small amounts of carbonates and sulfates. *Applied Geochemistry, 27*(6), 1202–1213. https://doi.org/10.1016/j.apgeochem.2012.02.032.

De Soto, I. S., Ayora, C., & Cuevas, J. (2018). Geochemical processes in compacted clay in contact with an acid landfill leachate: Laboratory experiments and modelling results. *Clay Minerals, 49*(3), 443–455. https://doi.org/10.1180/claymin.2014.049.3.07.

Francisca, F. M., & Glatstein, D. A. (2010). Long term hydraulic conductivity of compacted soils permeated with landfill leachate. *Applied Clay Science, 49*(3), 187–193. https://doi.org/10.1016/j.clay.2010.05.003.

Gao, S., Chapman, W. G., & House, W. (2009). Application of low field NMR T2 measurements to clathrate hydrates. *Journal of Magnetic Resonance, 197*(2), 208–212. https://doi.org/10.1016/j.jmr.2008.12.022.

Guyonnet, D., Gaucher, E., Gaboriau, H., Pons, C.-H., Clinard, C., Norotte, V., & Didier, G. (2005). Geosynthetic clay liner interaction with leachate: Correlation between permeability, microstructure, and surface chemistry. *Journal of Geotechnical and Geoenvironmental Engineering, 131*(6), 740–749. https://doi.org/10.1061/(asce)1090-0241(2005)131:6(740).

Hou, J., Li, J., & Chen, Y. (2017). Coupling effect of landfill leachate and temperature on the microstructure of stabilized clay. *Bulletin of Engineering Geology and the Environment.* https://doi.org/10.1007/s10064-017-1099-z.

JGJ 89-1992. (1993). *Technical standard for sampling of undisturbed soils*. Beijing: Ministry of Construction of China (In Chinese).

Li, J.-s., Xue, Q., Wang, P., & Liu, L. (2013a). Influence of leachate pollution on mechanical properties of compacted clay: A case study on behaviors and mechanisms. *Engineering Geology, 167*, 128–133. https://doi.org/10.1016/j.enggeo.2013.10.013.

Li, Z., Katsumi, T., Inui, T., & Takai, A. (2013b). Fabric effect on hydraulic conductivity of kaolin under different chemical and biochemical conditions. *Soils and Foundations, 53*(5), 680–691. https://doi.org/10.1016/j.sandf.2013.08.006.

Li, L., Chen, J., Huang, Y., & Dou, Z. (2016). Experimental investigation and numerical simulation of contaminant migration in the compacted clay containing artificial fractures. *Environmental Earth Sciences, 75*(2). https://doi.org/10.1007/s12665-015-5027-x.

Liu, T., & Hu, L. (2014). Organic acid transport through a partially saturated liner system beneath a landfill. *Geotextiles and Geomembranes, 42*(5), 428–436. https://doi.org/10.1016/j.geotexmem.2014.06.007.

Lu, H., Li, J., Wang, W., & Wang, C. (2015). Cracking and water seepage of Xiashu loess used as landfill cover under wetting–drying cycles. *Environmental Earth Sciences, 74*(11), 7441–7450. https://doi.org/10.1007/s12665-015-4729-4.

Nayak, S., Sunil, B. M., & Shrihari, S. (2007). Hydraulic and compaction characteristics of leachate-contaminated lateritic soil. *Engineering Geology, 94*(3–4), 137–144. https://doi.org/10.1016/j.enggeo.2007.05.002.

Ozcoban, M. S., Cetinkaya, N., Celik, S. O., Demirkol, G. T., Cansiz, V., & Tufekci, N. (2013). Hydraulic conductivity and removal rate of compacted clays permeated with landfill leachate. *Desalination and Water Treatment, 51*(31–33), 6148–6157. https://doi.org/10.1080/19443994.2013.769662.

Oztoprak, S., & Pisirici, B. (2011). Effects of micro structure changes on the macro behaviour of Istanbul (Turkey) clays exposed to landfill leachate. *Engineering Geology, 121*(3–4), 110–122. https://doi.org/10.1016/j.enggeo.2011.05.005.

Qiang, X., Hai-jun, L., Zhen-ze, L., & Lei, L. (2014). Cracking, water permeability and deformation of compacted clay liners improved by straw fiber. *Engineering Geology, 178*, 82–90. https://doi.org/10.1016/j.enggeo.2014.05.013.

SL 237–1999. (1999). *Specification of soil test*. Beijing: China Water Power Press (In Chinese).

Tian, H., Wei, C., Wei, H., Yan, R., & Chen, P. (2013). An NMR-based analysis of soil–water characteristics. *Applied Magnetic Resonance, 45*(1), 49–61. https://doi.org/10.1007/s00723-013-0496-0.

VanGulck, J. F., & Rowe, R. K. (2004). Evolution of clog formation with time in columns permeated with synthetic landfill leachate. *Journal of Contaminant Hydrology, 75*(1–2), 115–139. https://doi.org/10.1016/j.jconhyd.2004.06.001.

Xie, H., Chen, Y., Ke, H., Tang, X., & Chen, R. (2009a). Analysis of diffusion-adsorption equivalency of landfill liner systems for organic contaminants. *Journal of Environmental Sciences, 21*(4), 552–560. https://doi.org/10.1016/s1001-0742(08)62307-4.

Xie, H., Chen, Y., Zhan, L., Chen, R., Tang, X., Chen, R., & Ke, H. (2009b). Investigation of migration of pollutant at the base of Suzhou Qizishan landfill without a liner system. *Journal of Zhejiang University-Science A, 10*(3), 439–449. https://doi.org/10.1631/jzus.a0820299.

Xie, H., Chen, Y., Thomas, H. R., Sedighi, M., Masum, S. A., & Ran, Q. (2015). Contaminant transport in the sub-surface soil of an uncontrolled landfill site in China: Site investigation and two-dimensional numerical analysis. *Environmental Science and Pollution Research, 23*(3), 2566–2575. https://doi.org/10.1007/s11356-015-5504-5.

Xie, H., Zhang, C., Feng, S., Wang, Q., & Yan, H. (2018). Analytical model for degradable organic contaminant transport through a GMB/GCL/AL system. *Journal of Environmental Engineering, 144*(3), 04018006. https://doi.org/10.1061/(asce)ee.1943-7870.0001338.

Xue, Q., Li, J.-s., & Liu, L. (2013). Experimental study on anti-seepage grout made of leachate contaminated clay in landfill. *Applied Clay Science, 80-81*, 438–442. https://doi.org/10.1016/j.clay.2013.06.026.

Zhan, T. L. T., Guan, C., Xie, H. J., & Chen, Y. M. (2014). Vertical migration of leachate pollutants in clayey soils beneath an uncontrolled landfill at Huainan, China: A field and theoretical investigation. *Science of the Total Environment, 470-471*, 290–298. https://doi.org/10.1016/j.scitotenv.2013.09.081.